

1 **Daytime and nighttime aerosol soluble iron formation in clean**  
2 **and slightly-polluted moisture air in a coastal city in eastern**  
3 **China**

4 Wenshuai Li<sup>1,2</sup>, Yuxuan Qi<sup>1,2</sup>, Yingchen Liu<sup>1,2</sup>, Guanru Wu<sup>1,2</sup>, Yanjing Zhang<sup>1,2</sup>, Jinhui Shi<sup>3</sup>, Wenjun  
5 Qu<sup>1,2</sup>, Lifang Sheng<sup>1,2</sup>, Wencai Wang<sup>1,2</sup>, Daizhou Zhang<sup>4</sup>, Yang Zhou<sup>1,2</sup>

6 <sup>1</sup>Frontier Science Center for Deep Ocean Multispheres and Earth System (FDOMES) and Physical  
7 Oceanography Laboratory, Ocean University of China, Qingdao, Shandong, China.

8 <sup>2</sup>College of Oceanic and Atmospheric Sciences, Ocean University of China, Qingdao, Shandong, China.

9 <sup>3</sup>College of Environmental Science and Engineering, Ocean University of China, Qingdao, Shandong,  
10 China.

11 <sup>4</sup>Faculty of Environmental and Symbiotic Sciences, Prefectural University of Kumamoto, Kumamoto,  
12 Japan.

13  
14 *Correspondence to: Daizhou Zhang (dzzhang@pu-kumamoto.ac.jp) and Yang Zhou (yangzhou@ouc.edu.cn)*

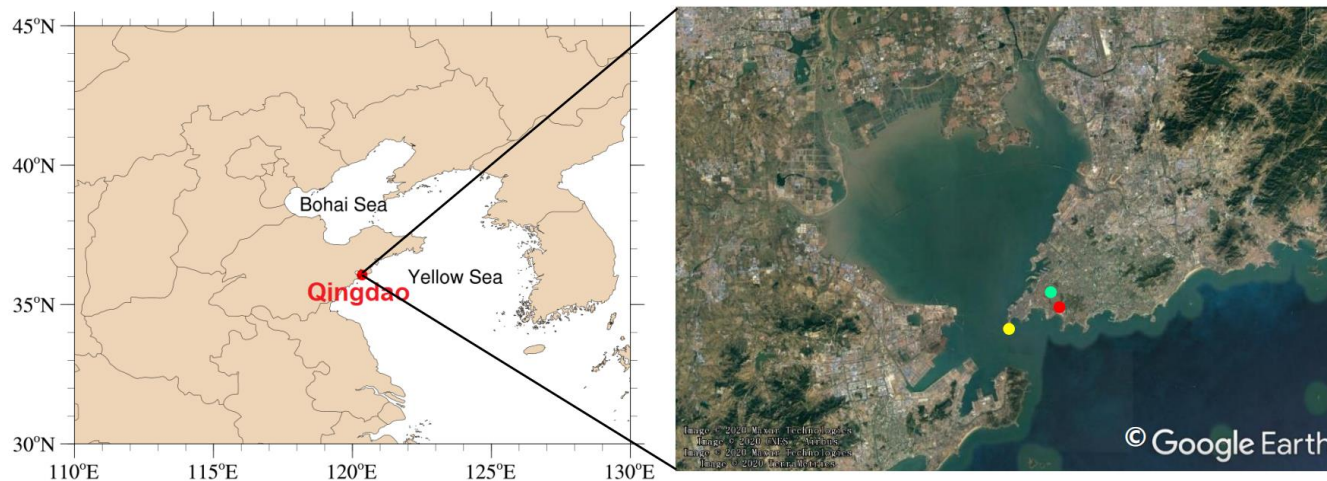
15  
16  
17  
18 **Contents of this file**

19 Figures S1 to S3

20 Tables S1 to S2

21

22



23 **Fig. S1.** Location of the sampling site. In the right panel, the red dot shows the location of the sampling  
24 site. The green dot shows the location of Qingdao Meteorological Bureau. The yellow dot shows the  
25 location of the air quality monitoring station in Qingdao (the west sub-station of the Shinan District).

26

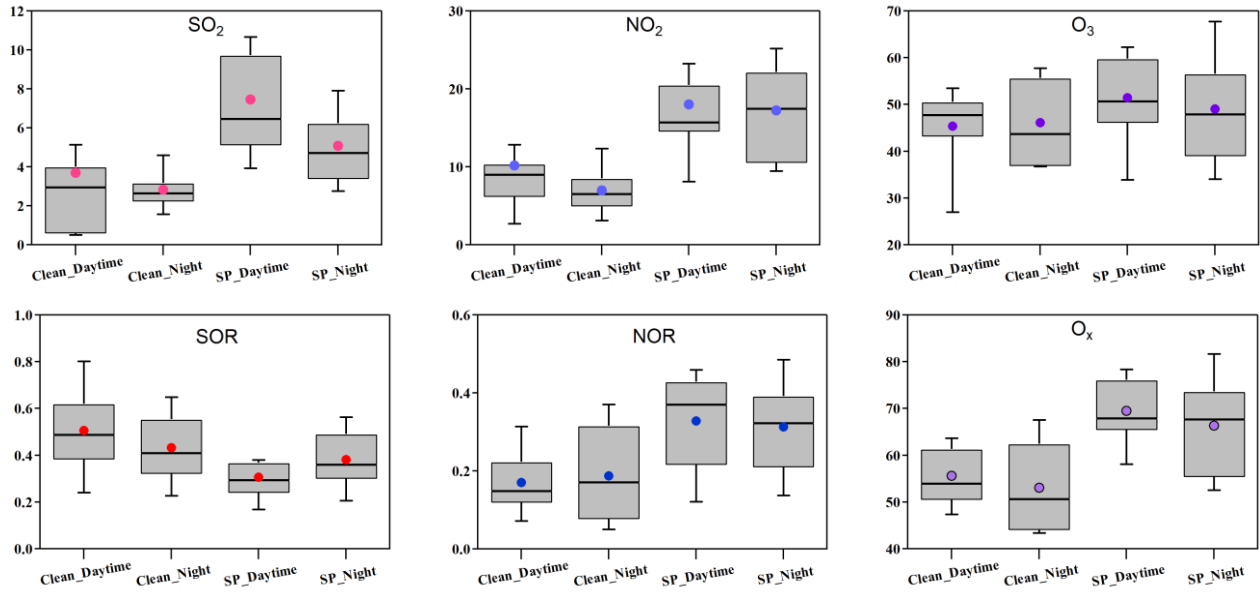
27

28

29

30

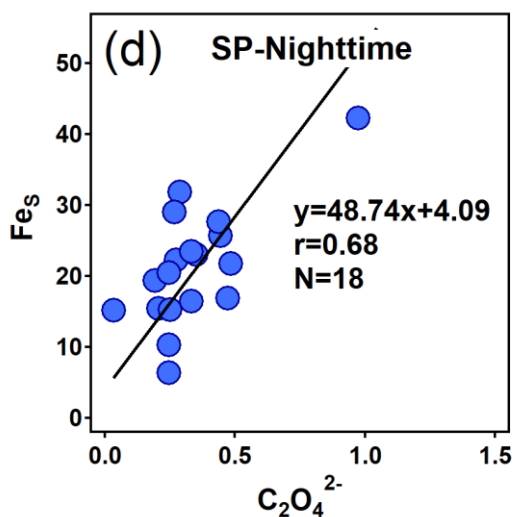
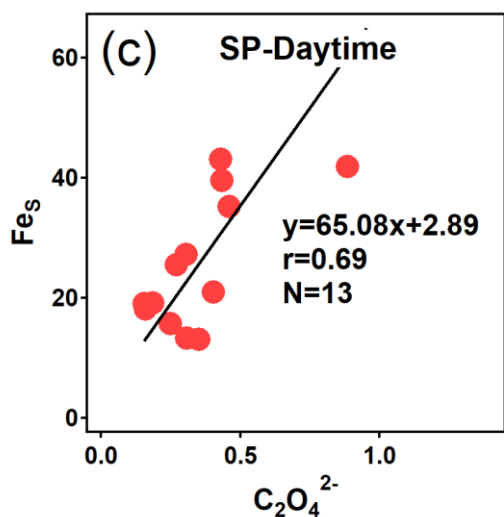
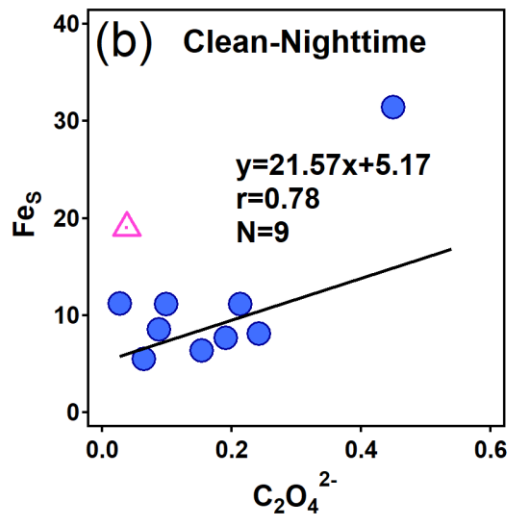
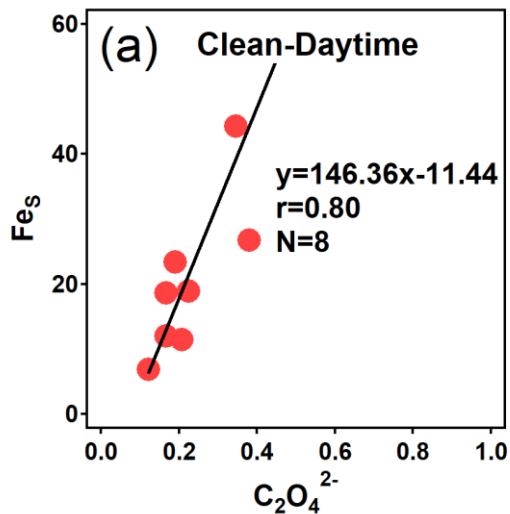
31



32 **Figure S2.** Box plots of several chemical parameters. Box and error bars represent the 25<sup>th</sup>, 50<sup>th</sup>, 75<sup>th</sup>, 10<sup>th</sup>,  
33 and 90<sup>th</sup> percentiles, respectively. The dots within the boxes represent the arithmetic means.

34

35



36

37

38 **Figure S3.** Relationships between soluble Fe ( $Fe_s$ , unit:  $ng\ m^{-3}$ ) and oxalate (unit:  $\mu g\ m^{-3}$ ). An extreme  
 39 point (marked by a pink triangle,  $\%Fe_s = 37.2\%$ ) in (b) was removed to obtain the more robust correlation  
 40 coefficient.

41

42 **Table S1.** Detection limits of the analysis instruments (unit:  $\mu\text{g L}^{-1}$  for WSIs and elements, and  $\mu\text{g}$  for  
 43 OC and EC).

Species	DL <sub>j</sub>	Species	DL <sub>j</sub>
Na <sup>+</sup>	20.0	V	0.0030
NH <sub>4</sub> <sup>+</sup>	20.0	Cr	0.0025
K <sup>+</sup>	10.0	Mn	0.0055
Mg <sup>2+</sup>	10.0	Fe	0.0139
Ca <sup>2+</sup>	20.0	Ni	0.0287
F <sup>-</sup>	10.0	Cu	0.0060
Cl <sup>-</sup>	40.0	Zn	0.0770
NO <sub>3</sub> <sup>-</sup>	10.0	As	0.0151
SO <sub>4</sub> <sup>2-</sup>	10.0	Se	0.4062
C <sub>2</sub> O <sub>4</sub> <sup>2-</sup>	10.0	Rb	0.0020
OC	0.20	Sr	0.0054
EC	0.20	Cd	0.0030
Al	0.0454	Ba	0.0022
Mg	0.0754	Pb	0.0026

44

45

46

**Table S2.** Classification results of aerosol samples.

Sample Types	Sample Number
Clean Periods Samples	19
Slightly-polluted Periods Samples	32
Heavily-polluted Periods Samples	6
Fog-impacted Samples	12
Dust-related Samples	70

47